Amino Acid Residues of *Escherichia coli* Acyl Carrier Protein Involved in Heterologous Protein Interactions†

Lesa M. S. Worsham,‡ Laurie Earls,‡ Carrie Jolly,‡ Keisha Gordon Langston,‡ M. Stephen Trent,§ and M. Lou Ernst-Fonberg*,‡

Department of Biochemistry and Molecular Biology and Department of Microbiology, James H. Quillen College of Medicine, East Tennessee State University, Johnson City, Tennessee 37614

Received May 28, 2002; Revised Manuscript Received November 15, 2002

ABSTRACT: Acyl carrier protein (ACP) is a small, highly conserved protein with an essential role in a myriad of reactions throughout lipid metabolism in plants and bacteria where it interacts with a remarkable diversity of proteins. The nature of the proper recognition and precise alignment between the protein moieties of ACP and its many interactive proteins is not understood. Residues conserved among ACPs from numerous plants and bacteria were considered as possibly being crucial to ACP's function, including protein−protein interaction, and a method of identifying amino acid residue clusters of high hydrophobicity on ACP's surface was used to estimate residues possibly involved in specific ACP−protein interactions. On the basis of this information, single-site mutation analysis of multiple residues, one at a time, of ACP was used to probe the identities of potential contact residues of ACPSH or acyl-ACP involved in specific interactions with selected enzymes. The roles of particular ACP residues were more precisely defined by site-directed fluorescence analyses of various myristoyl-mutant-ACPs upon specific interaction with the *Escherichia coli* hemolysin-activating acyltransferase, HlyC. This was done by selectively labeling each mutated site, one at a time, with an environmentally sensitive fluoroprobe and observing its fluorescence behavior in the absence and presence of HlyC. Consequently, a picture of the portion of ACP involved in selected macromolecular interaction has emerged.

Acyl carrier protein (ACP)[1] is a small (77 amino acids) protein that has an essential role in a myriad of metabolic pathways consequently entailing specific recognition of a remarkable diversity of proteins. Assorted functions involve fatty acid (*1*) and lipid biosynthesis (*2*), lipid A formation (*3*), membrane-derived oligosaccharide biosynthesis (*4*), and activation of RTX (repeats in toxin) toxins of Gram-negative bacteria (*5*). In particular instances, specialized ACPs operate in restricted pathways such as rhizobial nodulation signaling factors (*6*), polyketide antibiotics (*7*), and lipoteichoic acid synthesis (*8*).

Given its crucial roles in metabolism across the richness of life, the high degree of conservation of ACP's primary structure is not surprising. The three-dimensional structure of *Escherichia coli* ACP is the prototype of bacterial and plant ACP structures (*9*−*11*). Its solution structure consists of a three-helix bundle and a short fourth helix, all connected by loops with a long, structured turn between helices II and I. ACP's unusually mobile structure is best represented as a dynamic equilibrium of two conformers (*10*, *12*). Highly mobile portions include the loop regions and helix II. ACPs may be among the so-called intrinsically unstructured proteins (*13*) which are inherently flexible proteins lacking structure (to some degree) under physiologic conditions. Their conformations may be shaped through interactions with other macromolecules, an important capacity for proteins involved in cellular regulatory functions or to allow the ability to bind to assorted targets (*14*).

ACP was initially described as a substrate carrier in fatty acid biosynthesis. Two motifs of fatty acid synthase structure prevail in nature. In animals, the component enzymes and ACP are joined in peptide linkages to form a single, multifunctional polypeptide which dimerizes to form type I fatty acid synthase. In contrast, plants and most bacterial fatty acid synthases are isolated as discrete proteins containing individual catalytic functions, which act in concert to catalyze fatty acid biosynthesis, type II fatty acid synthase. The substrate is carried from one enzyme to the next as an acyl group bound in thioester linkage to the terminal S atom on ACP's 4′-phosphopantetheine prosthetic group that is covalently bound in phosphodiester linkage to the hydroxyl

† This work was supported by National Institutes of Health Grants R01-GM62121 and R15-GMOD54337 and a grant from the American Heart Association, Southeast Affiliate.

* To whom correspondence should be addressed. Phone: (423) 439−2025. Fax: (423) 439−2030. E-mail: ernstfon@etsu.edu.

‡ Department of Biochemistry and Molecular Biology.

§ Department of Microbiology.

[1] Abbreviations: RTX, repeats in toxin; proHlyA, hemolysin A protoxin; HlyA, hemolysin A toxin; HlyC, acyl-ACP-proHlyA acyltransferase; ACP, acyl carrier protein; ACPSH, acyl carrier protein with a free prosthetic group thiol; malonoyl-ACP, acyl carrier protein with a malonic acyl group covalently attached to the prosthetic group thiol; myristoyl−ACP, acyl carrier protein with a 14 carbon acyl chain covalently attached to the prosthetic group thiol; acyl-ACP, acyl carrier protein with a long chain fatty acyl chain covalently attached to the prosthetic group thiol; PIPES, piperazine-N,N′-bis(2-ethanesulfonic acid); HEPES, N-[2-hydroxyethyl]piperazine-N′-[2-ethanesulfonic acid]; EDTA, ethylenediaminetetraacetic acid; IPTG, isopropyl β-D-thiogalactopyranoside; SDS, sodium dodecyl sulfate; PAGE, polyacrylamide gel electrophoresis; PCR, polymerase chain reaction; MIANS, 2-(4′-maleimidylanilino)naphthalene-6-sulfonic acid, sodium salt; HPLC, high performance liquid chromatography.

10.1021/bi0261950 CCC: $25.00
Published on Web 12/13/2002

Table 1: Abilities of ACPSH Mutant to Participate in Biological Activities[a]

ACPSH mutant[b]	% of wild-type yield acyl-ACP synthase reaction[c]	% of wild-type ACPSH fatty acid synthase activity[d]	fatty acid synthase ACPSH K_m^{app} (μM)	fatty acid synthase ACPSH V_{max}^{app} (picomoles of [^{14}C]malonate incorporated/min[e])	% of wild-type ACPSH malonyl-CoA-ACP transacylase activity[f]	% of wild-type acyl-ACP-proHlyA acyltransferase activity[g]
wild-type	100	100 ± 8	4.4 ± 0.3	122 ± 4	100 ± 11	100 ± 9
V17C	88	55 ± 5	ND[h]	ND	63 ± 2	87 ± 7
N25C	105	155 ± 2	2.1 ± 0.1	178 ± 2	155 ± 9	109 ± 9
S27C	72	62 ± 1	4.4 ± 0.5	98 ± 4	134 ± 4	106 ± 5
V29C	133	81 ± 2	4.8 ± 0.5	106 ± 5	70 ± 3	74 ± 9
E30C	72	110 ± 0.1	5.7 ± 0.9	173 ± 13	56 ± 9	103 ± 7
G33C	42	39 ± 3	11 ± 1	133 ± 11	25 ± 5	71 ± 6
D35C	7	3 ± 2	ND	ND	4 ± 2	ND
L37C	12	9 ± 0.3	ND	ND	55 ± 1	ND
D38C	78	119 ± 4	ND	ND	162 ± 1	129 ± 19
E41C	88	12 ± 1	ND	ND	189 ± 1	84 ± 1
V43C	42	43 ± 5	9.6 ± 2	175 ± 18	22 ± 7	79 ± 3
E48C	100	86 ± 5	ND	ND	165 ± 4	96 ± 10
T52C	83	110 ± 3	7.9 ± 0.4	249 ± 6	102 ± 13	83 ± 6
I54C	67	45 ± 1	6.8 ± 0.9	40 ± 3	132 ± 2	83 ± 3
D56C	43	33 ± 0.3	8.0 ± 0.2	26 ± 0.3	131 ± 1	77 ± 3
K61C	32	47 ± 2	10.7 ± 1.5	76 ± 7	66 ± 5	85 ± 7
A68C	48	23 ± 4	4.0 ± 0.7	71 ± 6	35 ± 5	95 ± 8

[a] Procedures for acyl-ACP synthase reaction, malonoyl-CoA-ACP transacylase, fatty acid synthase, and acyl-ACP-proHlyA acyltransferase assays and kinetic methods are given in the Experimental Procedures. [b] Letters are one-letter amino acid abbreviations. [c] The yield of wild-type myristoyl-ACP was 60%, 1.8 mg of myristoyl-ACP from 3 mg ACPSH. [d] Wild-type ACPSH-supported fatty acid biosynthesis activity was 70 ± 2 pmol of [2-^{14}C]malonate incorporated/min with ACP (wild-type and mutants) at 6 μM. [e] Data are from 152 μg of fraction A/assay (*24*). [f] Wild-type ACPSH supported malonoyl-CoA-ACP transacylase activity was 186 ± 21 pmol of [2-^{14}C]malonate incorporated/min with all ACPs at 25 μM. [g] Under the assay conditions cited with all myristoyl-ACPs at 1μM, 8.4 pmol/min were transferred with wild-type myristoyl-ACP. [h] ND indicates not determined.

group of a serine residue (Ser 36 in *E. coli*) evolutionarily conserved among ACPs. The cofactor provides an extended arm upon which the reactive acyl moiety resides. In a type I fatty acid synthase, the arm conveys substrate among the anchored catalytic centers. In a type II fatty acid synthase, the arrival of the substrate into an enzyme active site follows the proper recognition and precise alignment between the protein moieties of ACP and the enzyme. After fatty acid biosynthesis, acyl-ACP is the essential acyl donor for many metabolic transfers of fatty acyl groups. For example, activation of *E. coli* hemolysin toxin (HlyA) by internal fatty acylation of two specific lysine residues of the protein protoxin (proHlyA) has an absolute requirement for acyl-ACP as the acyl donor (*5*, *15*). The reaction is catalyzed by an internal protein acyltransferase, HlyC. The nature of the specific recognition between ACP and its many interactive proteins is not understood.

Site-directed mutation analysis was used to identify ACP residues that might play a role in guiding ACPSH or acyl-ACP in specific interactions with selected enzymes. Selected residues were mutated, one at a time, to cysteine, a residue not present in wild-type *E. coli* ACP. The roles of mutated residues were more precisely defined by site-directed fluorescence analyses of various myristoyl-mutant-ACPs upon specific interaction with HlyC, an internal protein acyltransferase. Each mutated site was labeled with an environmentally sensitive fluoroprobe bound to the single SH group in myristoyl-mutant-ACP, and its fluorescence behavior observed in the absence and presence of HlyC. Accordingly a picture of the portion of ACP involved in selected macromolecular interaction has emerged.

EXPERIMENTAL PROCEDURES

Materials. [1-^{14}C]Myristate, [1-^{14}C]sodium pantothenate, and [2-^{14}C]malonoyl-CoA were from New England Nuclear. NADPH, NADH, malonoyl-CoA, and acetyl-CoA were from Sigma. *Eco*RV, *Dpn*-I, and Deep Vent DNA polymerase were from New England Biolabs. *Pfu Turbo* DNA polymerase was from Stratagene. 3-(1-pyridinio)-1-propanesulfonate was from Fluka. All chemicals were of reagent grade or better; organic solvents were of HPLC grade. Urea-containing buffers were freshly prepared. Ni-NTA agarose was from Qiagen. Novagen was the source of alkaline phosphatase conjugated S-peptide and pET plasmids. MIANS was from Molecular Probes.

Bacterial Strains and Growth Media and DNA. E. coli strains BLR(DE3)pLysS and BL21(DE3)pLysS were from Novagen, and XL-2 Blue was from Stratagene. Cells were grown in Luria broth except for expression of HlyC, which was obtained as described (*16*). A synthetic gene encoding the wild-type amino acid sequence of *E.* coli ACP subcloned into the plasmid pMR19 was a generous gift of Dr. John Cronan's laboratory (*17*−*19*). ACP was expressed from pMR19 in BLR(DE3)pLysS cells induced with 1 mM IPTG at A_{600nm} 0.6 and harvested after 18 h. Oligonucleotides for subcloning and site-directed mutagenesis of ACP were from Integrated DNA Technologies and are given in Supporting Information.

Site-Directed Mutagenesis. Site-directed mutations in the synthetic *ACP gene* were generated by the round circle PCR method described in the QuikChange Site-Directed Mutagenesis Kit protocol (Stratagene) using the plasmid pMR19 as the reaction template (*20*). The rationale involved whole-plasmid PCR amplification using the mutagenic oligonucleotides shown in Table 1, a 5′ and a 3′ primer for each mutation. Residual native plasmid was digested with the *dam* methylation-specific restriction endonuclease, *Dpn*-I, and the PCR product containing the mutation was transformed into XL2-Blue cells for efficient cloning of nonmethylated DNA. Mutation of DNA was confirmed by DNA sequence analysis

(*21*) at the Molecular Genetics Facility at the University of Georgia or the Molecular Genetics Core Facility, James H. Quillen College of Medicine, East Tennessee State University. Plasmids containing mutant ACPs were designated pMR19 along with a description of the mutation, and the vectors containing mutant ACPs were transformed into BLR-(DE3)pLysS for expression as described above for ACP.

Proteins. Proteins were handled at 4 °C unless noted otherwise. ProHlyA, ACPSH (wild-type and mutants), myristoyl−ACPs (wild-type and mutants), and [^{14}C]myristoyl−ACPs (wild-type and mutants) were prepared and purified as described by Trent and colleagues (*15*). [^{14}C]-ACPSH was made by adding 2 μM [1-^{14}C]sodium pantothenate, 5.4 Ci/M, (0.6 μCi) to 250 mL cultures of *E. coli* as we have previously described (*22*); the purified ACPSH had a specific radioactivity of 0.3 Ci/M. Myristoyl−ACPs (wild-type and mutants) were evaluated as described (*23*) and stored in aliquots at −80 °C. Preparation of HlyC expressed as a His_6-S-tag fusion protein from pTXC2 was done as described (*16*). Fatty acid synthase was isolated from *E. coli* (*24*).

Enzyme Assays. Fatty acid biosynthesis was measured as the incorporation of 2-[^{14}C]malonate into long chain fatty acids (*25*), and malonoyl-CoA-ACP transacylase activity was assayed as described (*23*). Activity of the internal protein acyltransferase HlyC was measured using the method of Trent and colleagues (*15*) and the HlyC and acylation substrate prepared as described (*16*). Fatty acid biosynthesis kinetic data was analyzed as previously described (*16*).

Protein Determination. Protein was measured by Bradford's method (*26*) except ACP and its derivatives, which were measured by the bicinchoninic acid protein assay (*27*).

Gel Electrophoresis, Western Blotting, and Fluorography. SDS−PAGE followed the procedure of Laemmli (*28*), and nondenaturing PAGE was done in the system devised by Post-Beittenmiller and colleagues (*29*). Coomassie blue staining was done using the reagent from Pierce. Fluorography of electrophoretic separations of radiolabeled proteins was done as we previously described (*15*). Gels and fluorograms were scanned and analyzed using Un-Scan-It (Silk Scientific) version 5.1.

Definition and Hydrophobicity Analysis of Clusters of Surface Amino Acid Residues. We thank Drs. Robert Jernigan (NCI, NIH, Bethesda, MD) and David Covell (SAIC, Frederick, MD) for performing the calculations on the surface of ACP to locate putative binding sites using the method that they described (*30*). The NMR solution structure of ACP was used for analysis (*9*).

Fluorescence Spectroscopy. (1) Steady-State Fluorescence and Anisotropy Measurements. Steady-State fluorescence measurements were made on a Perkin-Elmer 650-40 fluorescence spectrophotometer redesigned and rebuilt by On Line Instruments Systems, Inc., equipped with On Line Instruments Systems Spectroscopy Operating and Analysis Software, a T-type anisotropy measuring capability, stirrer, and thermostated (25 °C) cell holder. Spectra originated from data recorded at each nanometer, an average of 50 signals/datum. For steady-state fluorescence measurements, excitation was at 322 nm (7 nm band-pass) with emission measured between 350 and 550 nm (5 nm band-pass). Spectra were taken within 1−2 min of assembly of 1 mL of 25 mM Hepes (pH 8) containing 2 μM of the designated myristoyl-mutant-MIANS-ACP or 1 mL of 25 mM Hepes (pH 8) containing 2 μM myristoyl-mutant-MIANS-ACP + 10 μM HlyC. Spectra were repeated at 5−6 min after mixing of HlyC and myristoyl−ACPs with no changes being noted. Spectra that contained 2 μM ACPS-MIANS in differing 2-propanol % were prepared in 25 mM Pipes (pH 6.8). All spectra were corrected by subtracting the appropriate blanks obtained under identical instrument conditions and subjected to a 25 point least-squares quartic smooth using the software described above.

With emission set at 430 nm, excitation anisotropy was measured at 355 nm, an average of 60 data points/min, each an average of 15 signals (*31*). Bandwidths were 15 and 10 for excitation and emission, respectively.

(2) Preparation of MIANS-ACP Derivatives. MIANS stock solutions were freshly prepared in dimethyl sulfoxide (high purity, HPLC grade) and were handled and measured according to the manufacturer's instructions. ACPSH and myristoyl-mutant ACPs were prepared as described above, and for reaction with MIANS, were ∼100−200 μM in 25 mM Pipes (pH 6.8). Each ACP was reacted with a 10-fold excess of MIANS. Reactions of ∼500 μL were done in darkness at 4 °C in stirred Teflon-topped Reacti-Vials (Pierce). Dithiothreitol was added after 1 h to stop reaction. Reactions were dialyzed in darkness at 4 °C against three changes (overnight) of 250-fold excess of 25 mM Pipes (pH 6.8). The extent of reaction between MIANS and ACPSH or myristoyl-mutant-ACPs was measured using an A_{322} extinction coefficient of 27 000 in methanol for reacted MIANS (*32*); all samples were fully derivatized. The ACPS-MIANS and myristoyl-mutant C-MIANS-ACPs were stored below −20 °C.

(3) Stern−Volmer Quenching. Quenching experiments were performed with excitation at 322 nm, and emission monitored at the maximum wavelength (Table 3) of each MIANS conjugated ACP. Aliquots of freshly prepared 5.0 M acrylamide solution in 25 mM Pipes (pH 6.8) were added with stirring to 1.0 mL of 2 μM MIANS conjugated ACP; this was immediately followed by a duplicate determination except that 10 μM HlyC had been included in the solution 10 min prior to the measurements of acrylamide quenching. Relative fluorescence intensities were measured 2 min after acrylamide aliquot addition; using the data assay mode of the software described above, 60 measurements were averaged for 1 min, each an average of 30 signals. It was experimentally determined that no corrections were required for absorptive screening or dilution effects. Quenching results were plotted as the ratio of the fluorescence intensity in the absence of quencher (F_0) to the intensity in the presence of quencher (F) versus quencher concentration (Q). The collisional quenching process was measured according to the Stern−Volmer equation to ascertain $K_{SV,}$ the collisional quenching constant (*33*): $F_0/F = 1 + K_{SV}(Q)$. Linear plots were obtained with R-values greater than 0.97 in all cases except acyl-G33C-MIANS quenched in the presence of HlyC where the R-value could not be improved above 0.79.

RESULTS

Mutation of Selected Single Residues of ACPSH. There is little indication how ACP with its multiplicity of roles in diverse metabolic systems in microorganisms and plants

Table 2: Steady State Fluorescence of Myristoyl-Mutant-MIANS-ACP's with and without HlyC[a]

myristoyl-mutant-ACP MIANS residue location[b]	peak of maximum fluorescence (nm)	peak relative fluorescence yield	Δ nm blue shift upon HlyC addition	% change in relative fluorescence intensity upon HlyC addition
acyl-V17C	449	3.773	5	+22
acyl-N25C	450	3.797	3	−1
acyl-S27C	445	0.261	10	+165
acyl-V29C	450	1.632	11	+90
acyl-E30C	449	3.984	8	+25
acyl-G33C	448	0.213	12	+178
wild-type ACPSH[c]	449	3.044	11	+53
acyl-D38C	450	4.396	6	+9
acyl-E41C	452	0.9822	20	+162
acyl-V43C	448	2.073	12	+77
acyl-E48C	450	0.752	14	+99
acyl-T52C	450	0.399	8	+11
acyl-I54C	447	0.998	13	+62
acyl-D56C	450	0.845	15	+131
acyl-K61C	448	2.090	11	+83
acyl-A68C	451	1.898	11	+45

[a] Preparation of MIANS derivatives of ACPSH and myristoyl-mutant-ACPs and fluorescence spectroscoptic techniques are given in the Experimental Procedures; spectra that included 10 μM HlyC were taken 1−2 min after mixing of HlyC and myristoyl-mutant-MIANS-ACP or ACPS-MIANS. [b] Letters are one-letter amino acid abbreviations. [c] MIANS on prosthetic group on residue 36.

Table 3: Acrylamide Quenching of Myristoyl-Mutant-MIANS-ACPS with and without HlyC[a]

ACP MIANS source	$K_{SV-HlyC}$	$K_{SV+HlyC}$	$K_{SV-HlyC}/K_{SV+HlyC}$
acyl-V17C-MIANS	7.78 ± 0.15	7.77 ± 0.10	1.0 ± 0.02
acyl-N25C-MIANS	7.61 ± 0.07	6.58 ± 0.05	1.2 ± 0.01
acyl-S27C-MIANS	4.89 ± 0.01	2.30 ± 0.03	2.1 ± 0.03
acyl-V29C-MIANS	7.00 ± 0.15	4.43 ± 0.25	1.6 ± 0.10
acyl-E30C-MIANS	8.00 ± 0.16	4.81 ± 0.11	1.7 ± 0.05
acyl-G33C-MIANS	4.88 ± 0.01	1.42 ± 0.24	3.4 ± 0.58
wild-type ACPSH[b]	8.35 ± 0.27	4.73 ± 0.35	1.8 ± 0.15
acyl-D38C-MIANS	8.63 ± 0.12	4.09 ± 0.18	2.1 ± 0.10
acyl-E41C-MIANS	6.10 ± 0.08	4.63 ± 0.21	1.3 ± 0.06
acyl-V43C-MIANS	8.88 ± 0.08	6.01 ± 0.13	1.5 ± 0.04
acyl-E48C-MIANS	7.31 ± 0.23	5.35 ± 0.20	1.4 ± 0.07
acyl-K61C-MIANS	7.03 ± 0.03	6.39 ± 0.12	1.1 ± 0.02
acyl-A68C-MIANS	6.67 ± 0.07	6.91 ± 0.15	1.0 ± 0.02
acyl-I54C-MIANS	6.38 ± 0.17	4.73 ± 0.09	1.4 ± 0.04
acyl-D56C-MIANS	6.87 ± 0.28	5.40 ± 0.21	1.3 ± 0.07

[a] Preparation of MIANS derivatives of ACPSH and myristoyl-mutant-ACPs and quenching measurement methods are given in the Experimental Procedures. ACPs were 2 μM and HlyC was 10 μM. Letters are one-letter amino acid abbreviations. [b] MIANS was on the prosthetic group on residue 36. K_{SV} errors were the differences in the slopes of f_0/f plots of the fluorescence measurements uncorrected and corrected for sigma values. Following the addition of each aliquot of acrylamide, fluorescence was recorded as an average of 60 measurements/min, each an average of 30 signals, and the sigma values were calculated. The propagated errors of the K_{SV} ratios were computed from the two quenching constants and their standard deviations shown above for each MIANS labeled site.

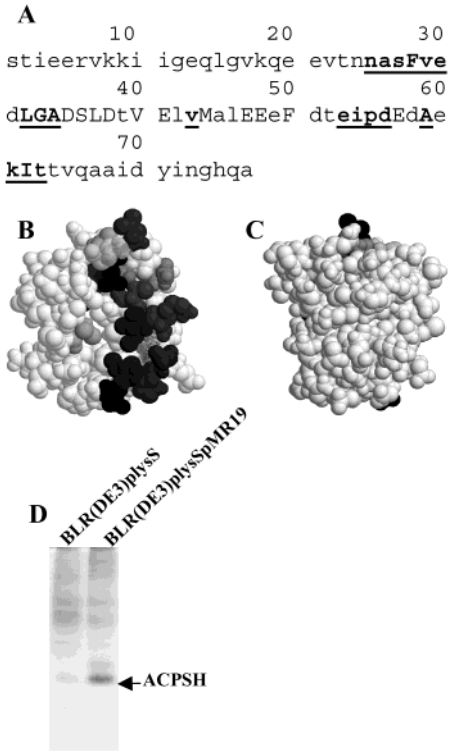

FIGURE 1: *E. coli* ACP structures showing potential interactive residues and ACP expression for mutational analysis. (A) ACP amino acid sequence showing in upper case letters residues conserved among ACPs from numerous plants and bacteria (*34*). Underlined residues in bold type were those predicted to be components of surface hydrophobicity clusters involved in protein−protein interactions. Surface hydrophobicity cluster analysis was done using the computational method summarized in the text (*30*). (B) Space filling model of the structure of *E. coli* ACP showing the side of the molecule containing the predicted binding sites. (C) Rotation, ~180° about the *y*-axis, of panel B view showing that the opposite side of ACP contained no predicted binding sites. Figures B and C were done using RasWin Molecular Graphics Windows Version 2.6. (D) Nondenaturing 13% PAGE analysis of induced expression of the synthetic ACP gene from pMR19 compared to the host cell, BLR(DE3)plysS, without pMR19; 6.75 μg of protein was loaded/lane.

recognizes and specifically interacts with many different proteins. Residues conserved among ACPs from numerous plants and bacteria (Figure 1A) (*34*) were considered as possibly being crucial to ACP's function, including protein−protein interaction. Also, a method of identifying amino acid residue clusters of high hydrophobicity on ACP's surface was used to estimate residues possibly involved in specific ACP−protein interactions. The three-dimensional structure of ACP (*9*) was analyzed (*30*) to determine clusters of surface-accessible amino acids, and each cluster was scored according to the hydrophobicity of its constituent amino acids. ACP's 10 most hydrophobic clusters of surface amino acids were not 10 independent locations. Instead, substantial overlaps among several groups of residues suggested two main surface areas, grouped on one face of the molecule, likely to be involved in protein−protein interaction. Residues that were designated in more than one cluster are shown

underlined in bold in the primary sequence (Figure 1A) and in their three-dimensional structure positions (Figure 1B). The opposite face of ACP was devoid of predicted binding sites (Figure 1C). Overlap is evident between conserved residues and residues predicted to be involved in protein−protein association. Such observations provided guidance for the selection of residues for mutation analysis.

The synthetic ACP gene contained in pMR19 was used as the source of wild-type and single-site mutations of ACP. Expression of host cell ACP was minimal, and upon transformation and expression of plasmid pMR19, the proportion of ACPSH in the soluble protein increased greatly (Figure 1D). The electrophoretic pattern of purified ACPSH showed negligible apo-ACP, which migrates more slowly than ACPSH. The band corresponding to holo-ACPSH was 95% of the staining protein, and the same band was depicted upon fluorography when ACPSH was isolated from cells grown in the presence of [^{14}C]pantothenate which labeled ACPSH's prosthetic group (shown in Supporting Information).

Ample yields of holo-ACP were obtained for most of the 17 different single site mutant ACPs. [^{14}C]Pantothenate incorporation into wild-type and each mutant provided an estimate of the proportion of holo-ACP and verified its PAGE migration location; nondenaturing PAGEs are shown in Supporting Information. D35C incorporated virtually no [^{14}C]pantothenate; it appeared as apo-D35C. I54C and D56C yields of holo-ACP were notably reduced. The remaining mutants and wild-type were estimated by scanning and analysis to be greater than 90% holo-ACP. Most of the mutants were obvious by their distinctive migration patterns upon nondenaturing PAGE compared to wild-type ACPSH. Generally, the mutant ACPs seemed to be somewhat structurally destabilized assuming a more open conformation resulting in slower migration than wild-type ACPSH. Exceptions were N25C, E41C, and T52C and to a lesser degree, E48C. These were all substitutions of a polar amino acid by another polar amino acid, cysteine, and their electrophoretic mobilities reflected more compact structures than wild-type ACPSH. The naturally occurring mutation of ACP where an isoleucine was substituted for valine at position 43 results in an ACP with a more compact structure (*35*). In contrast when the substitution at site 43 was a more polar residue, cysteine, decreased mobility indicated that the mutation resulted in a more open structure.

Myristoyl-ACP Mutants. Each of the single site mutated ACPs was subjected to myristoylation using acyl-ACP synthase as described in the Experimental Procedures, and all mutants except D35C and L37C were acylated to an appreciable extent (Table 1 and Supporting Information). The acylation reaction yields varied from 19 to 80% with 60% of wild-type being acylated under the conditions used. ACP mutants, other than D35C and L37C, which gave less than 45% of wild-type yield of myristoyl−ACP were G33C, V43C, D56C, and K61C. The lower yields may reflect effects of the single-site mutations causing less efficient substrates for the acyl-ACP synthase. The presence of the acyl-group has an organizing effect on the structure of wild-type ACP (*36*) and appeared to exert a similar effect upon most of the mutant ACPs. Generally, myristoylation of mutant ACPs created more compact structures that migrated faster than the corresponding ACPSHs. The mutation myristoyl-V17C with a slower migration than either wild-type or the unacylated V17C was an exception to this behavior; myristoylation made its conformation less compact.

Purified ACPSH Mutants as Fatty Acid Synthase Substrates. The single-site ACPSH mutants generally either supported fatty acid biosynthesis to the same extent as wild-type ACPSH or to a lesser extent (Table 1). One of two exceptions was the ACP mutant N25C that supported fatty acid biosynthesis at 155% the rate of wild-type. Under the conditions given, wild-type K_m^{app} and V_{max}^{app} were 4.4 ± 0.3 μM and 122 ± 4 pmol [^{14}C]malonate incorporated/min respectively; those of N25C were 2.1 ± 0.1 and 178 ± 2, respectively, a decreased K_m^{app} and a higher V_{max}^{app} which led to enhanced activity. Less than half of wild-type fatty acid biosynthetic activity was supported by G33C even though it appeared to be largely holo-ACP; kinetic analysis of G33C showed a 2.6-fold increase in K_m^{app} with V_{max}^{app} practically unchanged. In contrast, S27C mutant decreased support of fatty acid synthase activity stemmed from a decreased V_{max}^{app} while K_m^{app} was unchanged compared to wild-type. D35C which lacked a 4′-phosphopantetheine prosthetic group was inactive; the infinitesimal activity seen likely stemmed from the wild-type ACPSH present in the host cell. L37C showed almost no support of fatty acid biosynthesis at 9% of wild-type activity, even though it was greater than 90% holo-ACP. Of the remaining mutants with greater than 50% reduction in support of fatty acid biosynthesis, E41C, V43C, I54C, D56C, K61C, and A68C, kinetic analyses of V43C, D56C and K61C showed approximate doubling of K_m^{app} values; V_{max}^{app} values of D56C and K61C were reduced while that of V43C increased but not enough to overcome the depression in rate caused by the increased K_m^{app}. I54C and A68C mutants had reduced V_{max}^{app} values.

The effectiveness of the ACPSH mutants in supporting *E. coli* malonyl-CoA-ACP transacylase activity, a component activity of fatty acid biosynthesis, resembled the support of fatty acid biosynthesis for about half of the mutants (Table 1). Compared to wild-type ACPSH, E30C, and V43C were less effective in supporting the transacylase activity than in supporting fatty acid synthase activity. Thus malonyl-transacylase activity was not rate limiting in fatty acid biosynthesis since it was impaired with less than ideal substrates while fatty acid biosynthesis was unaffected or less affected. ACPSH mutants S27C, D38C, E41C, E48C, I54C, and D56C supported malonyl-transacylase activity to a greater extent than did wild-type ACPSH and, along with L37C, were more effective in supporting transacylase activity than fatty acid biosynthesis. Mutation to cysteine of either residue Asp35 or Leu37, which flank Ser36, the site of 4′-phosphopantetheine attachment, resulted in no support of malonyl-transacylase activity by D35C while L37C supported half the wild-type malonyl transacylase activity.

Myristoyl-ACP Mutants as Acyl Donors for Hemolysin Activation. HlyA, a toxic protein secreted by pathogenic *E. coli*, arises, as stated above, from nontoxic proHlyA by HlyC-catalyzed posttranslational, internal protein fatty acylation from acyl-ACP, the required acyl donor (*5*, *15*). The effects of different single site mutations of ACP on myristoyl−ACP's performance in proHlyA activation to HlyA were examined (Table 1). In contrast to fatty acid biosynthesis and malonyl-CoA-ACP transacylase activities, none of the mutants supported a markedly increased rate of reaction

compared to wild-type. Myristoyl−ACP mutants that resulted in less than 80% of wild-type acyl-donor efficacy were V29C, G33C, V43C, and D56C; these mutants also showed depressed support of fatty acid biosynthesis and, except D56C, malonyl-transacylase activity.

Fluorescence Spectroscopy of MIANS-ACP Compounds. MIANS, a fluorescent derivative of maleimide, is nonfluorescent until it reacts with a thiol, and it reacts quickly with protein thiols where its fluorescence is very sensitive to the hydrophobicity of the environment (*32*). Its fluorescence behavior in proteins exhibits high sensitivity to ligand binding and protein association, but its absorbance is not affected by environmental polarity (*37*). The single thiol of wild-type ACPSH located on the prosthetic group was reacted with MIANS as described in the Experimental Procedures. The fluorescence behavior of ACPS-MIANS in solutions containing different percentages of 2-propanol was observed following excitation at 322 nm. ACPS-MIANS emitted fluorescence in the range of 400−460 nm, and its fluorescent properties depended upon the polarity of the environment. The wavelength of maximum fluorescence and relative fluorescence intensity varied in response to the percentage of 2-propanol in the medium. As the percentage of 2-propanol changed from 0 to 90, the fluorescence emission increased ∼12-fold; at the same time the position of the maximum wavelength shifted 30 nm from 450 to 420. These findings showed that MIANS labels strategically placed within ACP were potentially useful indicators of the microenvironment within the protein and of changes that might occur in the microenvironment of the probe upon heterologous protein interaction with ACP.

Fluorescence anisotropy is an independent method to detect a fluorescent protein's participation in complex formation providing that temperature and solvent are invariant. This technique is based on molecular size changes and is responsive to molecular associations even when the fluorescence spectrum and relative fluorescence intensity are unaffected. The measured anisotropy r is related to the fluorescence lifetime τ and to φ, the rotational correlation time of the fluorophore, by the following equation in which r_o is a property of the fluorophore, $r = r_o/(1 + (\tau/\varphi))$. The value of φ of the molecule to which the fluorophore is attached is directly related to the volume V of the molecule (or the complex in which it is contained); $\varphi = nV/RT$ (*31*). Complex formation results in change in macromolecular size (V) and appears as an altered rotational correlation time affecting the observed anisotropy.

The thiol located on the cysteine residue of a mutant myristoyl−ACP, myristoyl-V29C, was reacted with MIANS as described in Experimental Procedures. The anisotropy of 2 μM myristoyl-V29C-MIANS was 0.0583 ± 0.014; upon addition of 10 μM HlyC, the anisotropy increased over 3-fold to 0.1920 ± 0.011 indicating complex formation between MIANS-labeled myristoyl−ACP (9057 Da) and HlyC (22 384 Da), a change in macromolecular size from 9057 to 31 441 daltons. Addition of 10 μM of a nonreactive protein, ACPSH, to 2 μM myristoyl-V29C-MIANS did not result in a change in anisotropy of the solution corroborating that the anisotropy increase occurred in response to specific complex formation. Thus, specific interaction in solution between myristoyl−ACP and the acyltransferase HlyC in the absence of the ultimate acyl acceptor, prohemolysin, was confirmed (*16*).

Site-Directed Mutation-Fluorescence Spectroscopic Analysis of Myristoyl-ACPs. As shown above, the fluorescence response of a MIANS fluorophore attached to the thiol group in ACPSH depended upon its environment. Accordingly, a MIANS group was moved to different locations in myristoyl−ACP via the mutagenic generation of cysteine residues at different sites, one at a time. Prior to treatment with MIANS, each mutant ACP was myristoylated as described above. Consequently, one sulfhydryl group was available for bonding with MIANS in each of the mutants where a single residue was mutated to a cysteine residue. The acyltransferase HlyC, shown above to interact with myristoyl−ACP, was used for site-directed fluorescence study of ACP's specific interaction with another protein. Other enzymes examined herein used ACPSH as substrate, which upon site-directed mutation generation of cysteine residues would have presented two thiol groups for MIANS reaction, cysteine and the sulfhydryl group on the phosphopantetheine prosthetic group. Reaction of multiple thiols with MIANS would have complicated experimental interpretation.

The fluorescence spectra of myristoyl-mutant-ACPs all had about the same maximum wavelength, ∼450 nm, but the relative fluorescence yields varied depending on the location of the label in the three-dimensional structure (Figure 2). The fluorescence emission maxima and relative fluorescence yields for mutants and wild-type MIANS derivatives are given in Table 2. Addition of 10 μM HlyC frequently resulted in significant alterations of the properties of a particular myristoyl-mutant-MIANS-ACP (Table 2). Myristoyl−ACP mutants V17C, N25C, E30C, D38C, and T52C did not exhibit large changes in fluorescence characteristics upon the addition of an excess of HlyC. ACP mutants D35C and L37C were not examined. The remaining myristoyl−ACP-MIANS mutants and wild-type ACPS-MIANS fluorescence changes indicated an altered residue microenvironment upon the addition of HlyC. The changes in fluorescence characteristics were consistently an increase in relative fluorescence yield accompanied by a blue shift in the peak of maximum fluorescence. Figure 3A shows an example of the lack of change in fluorescence behavior seen with myristoyl-N25C-MIANS-ACP without and with HlyC compared with an example of marked changes seen with myristoyl-E41C-MIANS-ACP under similar conditions (Figure 3B). The following myristoyl−ACP mutants showed a 12 nm or greater blue shift in fluorescence maximum and/or greater than a 70% increase in relative fluorescence upon addition of HlyC to the following solutions: S27C, V29C, G33C, E41C, V43C, E48C, I54C, D56C, and K61C. Wild-type ACPS-MIANS and myristoyl-A68C-MIANS-ACP exhibited slightly lesser changes.

Acrylamide is a polar, uncharged molecule that quenches fluorescence predominately by a collisional process, and the degree of quenching by acrylamide is sensitive to the accessibility of a fluorescent label in proteins. The accessibility of MIANS fluorophore attached at different sites throughout ACP was determined by quenching its fluorescence with acrylamide; this was done in the absence and presence of HlyC. The collisional quenching process was measured as described above to determine the values of K_{SV}, the collisional quenching constant. The values of K_{SV} were measured for MIANS-labeled myristoylated mutants and wild-type ACPS-MIANS in the absence and presence of

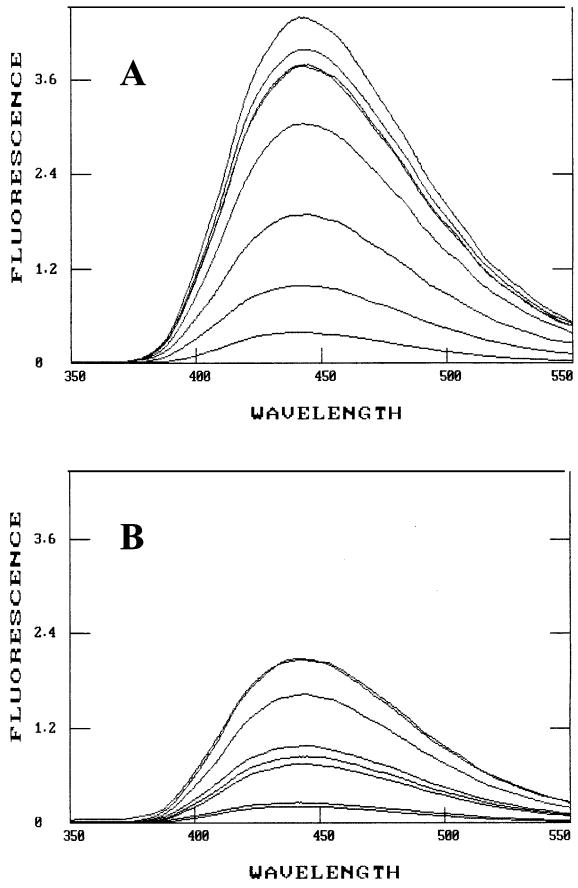

FIGURE 2: Steady-state fluorescence spectra of *E. coli* ACP-MIANS derivatives. Eight spectra of diverse ACP-MIANS preparations are present in each portion of the figure. Details of preparation of MIANS derivatives and fluorescence spectroscopy are given in the Experimental Procedures. Each ACP contained one thiol group reacted with the fluoroprobe MIANS. Wild-type was ACPS-MIANS. The others were myristoyl−ACPs where each ACP had a different site mutated to a cysteine residue that was reacted with MIANS resulting in fluoroprobes at various locations throughout the molecule. Each spectrum was of 2 μM ACP in 25 mM Hepes (pH 8.0); the different relative fluorescence intensities of the spectra stemmed from the different environments of the fluoroprobe in various sites throughout the molecule. (A) From top to bottom, the spectra are of the following mutant myristoyl-MIANS-ACPs or wild-type ACPS-MIANS: D38C, E30C, N25C overlapping with V17C, wild-type, A68C, I54C, and T52C. (B) From top to bottom, the spectra are of the following mutant myristoyl-MIANS-ACPs: K61C and V43C overlapping, V29C, E41C, D56C, E48C, S27C, and G33C.

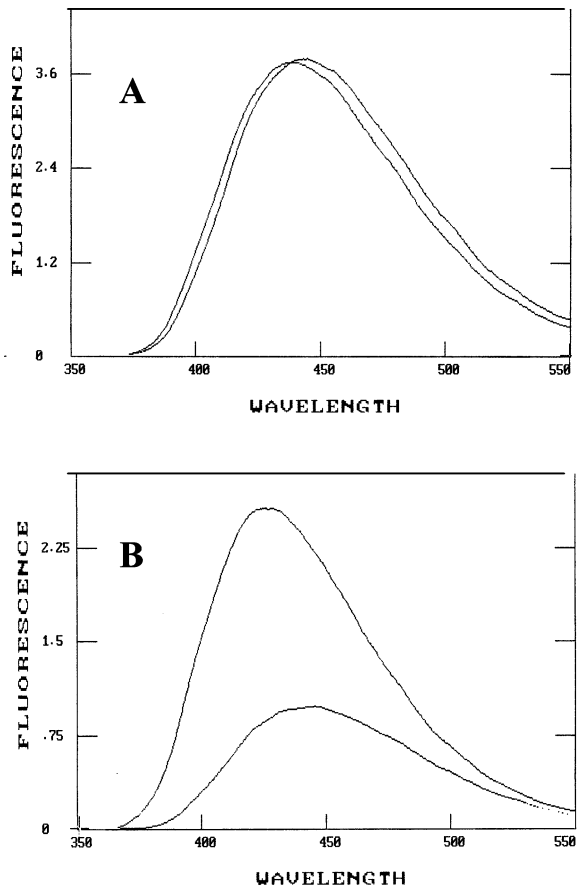

FIGURE 3: Steady-state fluorescence spectra of N25C (A) and E41C (B) with and without HlyC. Details of preparation of MIANS derivatives and fluorescence spectroscopy are given in the Experimental Procedures. Each ACP moiety was present at 2 μM. HlyC, 10 μM, was added, and spectra were taken 1−2 min after mixing. Blue shifted spectra in panels A and B are those where HlyC was present.

HlyC (Table 3). The quenching constant in the absence of HlyC was a measure of the ease with which acrylamide could access the fluoroprobe in its various sites within different myristoyl−ACP mutants, and most K_{SV} values were close to 7 or 8; myristoyl-S27C-MIANS-ACP, myristoyl-G33C-MIANS-ACP, and myristoyl-E41C-MIANS-ACP with K_{SV} values close to 5 or 6 were exceptions suggesting that these labeled residues were sterically less accessible to acrylamide than the others. Labeled myristoyl−ACP mutants that underwent the largest changes in K_{SV} upon addition of HlyC were myristoyl-S27C-MIANS-ACP, myristoyl-V29C-MIANS-ACP, myristoyl-E30C-MIANS-ACP, myristoyl-G33C-MIANS-ACP, myristoyl-D38C-MIANS-ACP, myristoyl-V43C-MIANS-ACP, and wild-type ACPS-MIANS. Those experiencing the next largest changes were myristoyl-V41C-MIANS-ACP, myristoyl-E48C-MIANS-ACP, and myristoyl-D56C-MIANS-ACP. Of these residues, myristoyl-E30C-MIANS-ACP, myristoyl-D38C-MIANS-ACP, and wild-type ACPS-MIANS were not among those showing the largest increases in fluorescence yield and blue shifts upon addition of HlyC to the ACP solution. Likely shielding of these residues from acrylamide access by HlyC interacting with nearby demonstrated contact residues is discussed below.

DISCUSSION

ACPSH mutation D35C resulted in virtually no holo-ACP formation; I54C and D56C showed impaired holo-ACP formation. In the homologous ACP from *Bacillus subtilis*, residue D35 is implicated in cocrystal structures in interactions between apo-ACP and holo-ACP synthase along with several other residues including D48, I54, and D56 (*38*). Reduced fatty acid biosynthesis for ACPSH mutants D35C, I54C, and D56C (Table 1) presumably stemmed, at least in part, from reduced holo-ACP formation. *E. coli* ACP residues predicted by computational analysis to be involved in docking with the fatty acid biosynthetic enzyme β-ketoacyl-ACP synthase III (FabH) are R6, E13, S36, E41, M44, A45, E47, E48, and E49 (*34*), and ACP residues implicated by NMR chemical shift perturbation to mediate interaction with a dehydrase (FabA) are N25, S36, D38, E41, E47, E53, E60, V40, and A45 (*39*). ACP residue E41 is a proposed interaction site with both of the enzymes cited above, and

ACPSH mutant E41C fatty acid synthase activity was greatly reduced (Table 1). Another ACPSH residue whose biological performance was affected by mutation to cysteine, N25, (Table 2) is also implicated as a contact residue in FabA interaction (*39*).

Interactive protein contact in the vicinity of a bound fluoroprobe on ACP would be expected to alter its environment, likely to a more hydrophobic one with increased shielding from the aqueous medium. An increase in the hydrophobicity of the environment of ACPS-MIANS equivalent to 10% 2-propanol led to an 84% increase in fluorescence yield accompanied by a blue-shift of ~10 nm. The MIANS responses upon HlyC binding to myristoyl−ACP, as MIANS was moved via single-site mutagenesis about ACP, varied from no change in relative fluorescence intensity to increases of greater than 100% and changes in the wavelength of maximum fluorescence ranged from blue shifts of 3 nm to as much as 20 nm (Table 2).

HlyC's interaction pattern on myristoyl−ACP's surface was outlined by the sites of MIANS labels throughout ACP whose environments were significantly changed upon the addition of HlyC (Table 2 and Figure 4, panels A, C, and E). ACPs bearing MIANS groups on residues not involved in interaction with HlyC (Figure 4, panels B, D, and F) did not demonstrate much change in fluorescence characteristics upon the addition of HlyC. Of the 16 different locations of the cysteine-MIANS label in myristoyl-mutant-ACPs (Figure 4, panels G and H), the following nine residue positions experienced, upon the addition of HlyC, fluorescence maximum changes of ≥12 nm blue shift and/or >70% increase in relative fluorescence intensity: S27C, V29C, G33C, E41C, V43C, E48C, I54C, D56C, and K61C. The alteration in residue microenvironment could stem from either a change in myristoyl-MIANS-ACP's conformation induced by HlyC binding or direct interaction with HlyC causing a change in fluoroprobe environment. Since, however, all fluorescence changes were unidirectional, increased relative fluorescence yield and blue shift of peak maximum, it is likely that the changes reflected contacts between MIANS groups and HlyC rather than conformational changes. Fluorescence changes secondary to conformational shifts remote from sites of HlyC/ACP contact would likely be of variable directions among different MIANS sites, that is red and blue shifts accompanying increased and decreased fluorescence yields. Furthermore, the affected residues included the same mutations that affected fatty acid synthase and HlyC activities. Several of these ACP residues are among those reported to interact with FabH, FabA, holo-ACP synthase, and covalently bound acyl-chain (*34*, *38*, *39*). Residues uniquely affected in observations reported here were S27C, V29C, G33C, V43C, and K61C.

Myristoyl-MIANS-ACP mutants that exhibited maximum fluorescence changes were among those showing HlyC-dependent changes in quenching with the exception of K61C, which showed little change in quenching constant (Table 3). K61C protrudes from the molecular surface and may be accessible from multiple sides of the molecule (Figure 4, panels G and H). Myristoyl-V17C-MIANS-ACP, which showed no change in fluorescence characteristics or acrylamide quenching upon addition of HlyC, is located on a different face of the molecule than residues implicated in intermolecular interactions (Figure 4H). Myristoyl−ACP

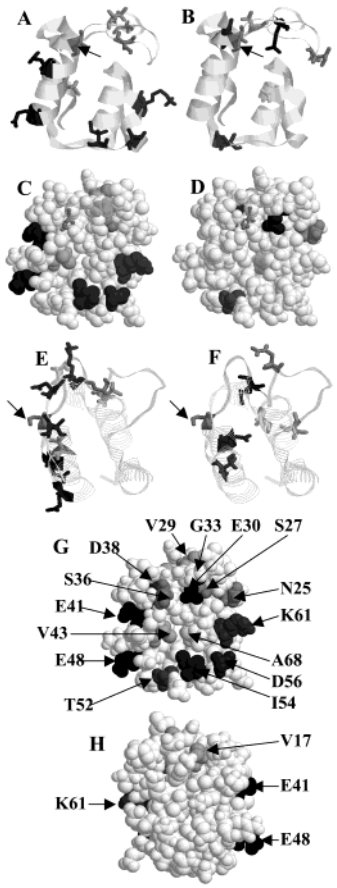

FIGURE 4: Three-dimensional structure locations of *E. coli* ACP sites of single mutations and designation of interactive and noninteractive MIANS-bound mutant residues of myristoyl−ACP. Interactive and noninteractive residues were determined by site-directed fluorescence analysis as described in the text. Panels A, B, C, D, and G are the same view of the molecule, and panel H is the rear of this aspect, turned 180 degrees on the *y*-axis. Panels E and F are ~90° rotations to the left of vistas A, B, C, and D. Panels A and B stick residues show interactive and noninteractive MIANS sites respectively within ACP's secondary structure; arrows indicate Ser36, the site of prosthetic group attachment. Panels C and D shaded residues show interactive and noninteractive sites respectively in a space-filling model; the site of the prosthetic group attachment (Ser36) is shown in ball-and-stick form in panels C and D. Panels E and F stick residues show interactive and noninteractive MIANS sites respectively; the site of the prosthetic group attachment, indicated by an arrow, is shown for reference in panels E and F. Panels G and H space filling models of opposing faces of ACP show all residues mutated, one at a time, and subjected to site-directed fluorescence analysis and biological activities assessments. Figures were done using RasWin Molecular Graphics Windows Version 2.6.

mutant residues that did not show significant changes in fluorescence characteristics upon addition of HlyC but had notable K_{SV} changes in response to HlyC were E30C-MIANS, D38C-MIANS, and wild-type ACPS-MIANS. These residues exist in the tertiary structure among residues implicated by fluorescence and activity changes to be involved in binding HlyC. This is seen in Figure 4D where Ser 36 (wild-type ACPS-MIANS) shown as ball-and-stick has E30C on its right side and D38C barely showing on its left. Comparison with implicated contact residues and Ser 36 as reference in Figure 4C suggests that HlyC juxtaposed to this face of myristoyl−ACP could have shielded these residues (E30C, Ser36 prosthetic group, and D38C) to some extent and restricted acrylamide access to them even though

they were not implicated to be contact residues. The single-site ACP mutations in question, E30C and D38C, did not affect ACP's biological activities. Residues implicated by fluorescence and activity changes to be involved in binding HlyC are grouped around the prosthetic-group-containing residue, Ser36, on one side of the three-dimensional structure (Figure 4C). The interactive residues of myristoyl−ACP (Figure 4, panels A, C, and E) are situated mostly on helix II or the structured portion (residues 26−34) of the loop between residues 15 and 35, regions of notable conformational mobility in an unusually mobile protein (*9*, *11*, *12*). The positions in the three-dimensional structure of residues which were evidently not involved in the macromolecular interactions examined are shown in Figure 4, panels B and D, identical molecular views as those shown in panels A and C. Generally, these residues do not appear to be as surface-accessible as those residues implicated in interaction. Figure 4E, a side view of the image in A, B, C, and D, illustrates clustering of the putative HlyC-recognition residues of ACP on two facets of the three-dimensional structure. Figure 4F, an identical perspective of the molecule, shows that residues which did not show fluorescence evidence of HlyC interaction were more randomly dispersed. Ser36 is shown as a point of reference in Figure 4, panels C, D, E, and F. Figure 4, panels A and B provide secondary structural orientation.

Complex formation with HlyC appeared to occur predominately on one face of myristoyl−ACP (Figure 4C). The appearance is one of the contacts distributed about ACP's surface encircling the covalent binding region at the S atom on ACP's prosthetic group thus strategically positioning the acyltransferase HlyC for catalysis (Figure 4, panels A, C, and E). This conjecture explains the fluorescence and quenching changes with and without HlyC observed for the wild-type ACPS-MIANS, where the environment of the MIANS bound not to a contact residue but to the terminal S atom of the prosthetic group undergoes considerable change upon the addition of HlyC (Tables 2 and 3). This change included a 53% increase in relative fluorescence, 11 nm blue shift of fluorescence maximum, and a large decrease in the ability of acrylamide to quench the MIANS located on the prosthetic group. These changes are consistent with a potentially interactive molecule positioning itself adjacent to the prosthetic group thus altering the environment of the prosthetic group thiol region and its access to acrylamide from the solvent. This model of prosthetic group behavior is consistent with that shown by NMR solution structure of the homologous ACP from *Mycrobacterium tuberculosis* (*13*).

About 40−50% of the ACP residues implicated herein to be directly involved in interactions with heterologous macromolecules overlap with those named to be so involved in other studies of ACP-macromolecular recognitions employing different methods (*34*, *39*, *40*). Of the nine residues identified by site-directed fluorescence to be involved in intermolecular interactions, seven were among those predicted in the hydrophobic surface cluster analysis (Figure 1). Assessments of the effects of single site-mutations of ACP on several of its biological functions showed 14 of the 17 sites selected for mutation to be adversely affected by mutation. Of these, nine were predicted binding residues by hydrophobic surface cluster analysis. Mapping of ACP's interaction with other proteins using different assessments of single-site mutation analysis has provided a picture of ACP-heterologous protein interaction.

ACKNOWLEDGMENT

We acknowledge with gratitude and pleasure our introduction to acyl carrier protein by Professor Konrad Bloch whose memory we revere.

SUPPORTING INFORMATION AVAILABLE

A table giving the primers used to construct the ACP mutants and a figure illustrating the expression, isolation, and myristoylation of purified ACPSH wild-type and single site mutations analyzed by nondenturing PAGE using Coomassie Blue staining and fluorography measuring incorporation of either [^{14}C]pantothenate into ACPSH or [^{14}C]myristate into myristoyl−ACP. This material is available free of charge via the Internet at http://pubs.acs.org.

REFERENCES

1. Rock, C. O., Jackowski, S., and Cronan, J. E., Jr. (1996) in *Biochemistry of Lipids and Lipoproteins and Membranes* (Vance, E. E., and Vance, J., Eds.) pp 35−74, Elsevier, Amsterdam.
2. Rock, C. O., and Jackowski, W. (1982) *J. Biol. Chem. 257*, 10759−10765.
3. Raetz, C. R. H. (1996) *Escherichia coli and Salmonella: Cellular and Molecular Biology*, American Society for Microbiology, Washington, DC.
4. Tang, L., Weissborn, A. C., and Kennedy, E. P. (1997) *J. Bacteriol. 179*, 3697−3705.
5. Issartl, J.-P., Koronakis, V., and Hughes, C. (1991) *Nature 351*, 759−761.
6. Geiger, O., Spaink, H. P., and Kennedy, E. P. (1991) *J. Bacteriol. 173*, 2872−2878.
7. Shen, B., Summers, R. G., Gramajo, H., Bibb, M. J., and Hutchinson, C. R. (1992) *J. Bacteriol. 174*, 3818−3821.
8. Heaton, M. P., and Neuhaus, F. C. (1994) *J. Bacteriol. 176*, 681−690.
9. Kim, Y., and Prestegard, J. H. (1989) *Biochemistry 28*, 8792−8797.
10. Kim, Y., and Prestegard, J. H. (1990) *Proteins: Struct. Funct. Genet. 8*, 377−385.
11. Fowler, C. A., Tian, F, Al-Hashimi, H. M., and Prestegard, J. H. (2000) *J. Mol. Biol. 304*, 447−460.
12. Andrec, M. R., Hill, R. B., Prestegard, J. H. (1995) *Protein Sci. 4*, 983−993.
13. Wong, H. C., Liu, G., Zhang, Y.-M., Rock, C. O., Zheng, J. (2002) *J. Biol. Chem. 277*, (in press).
14. Wright, P. E., and Dyson, H. J. (1999) *J. Mol. Biol. 293*, 321−331.
15. Trent, M. S., Worsham, L., Ernst-Fonberg, M. L. (1998) *Biochemistry 37*, 4644−4652.
16. Worsham, L. M. S., Trent, M. S., Earls, L, Jolly, C., and Ernst-Fonberg, M. L. (2001) *Biochemistry 40*, 13607−13616.
17. Cronan, J. E., Jr., Narashimhan, M. L., and Rawlings, M. (1988) *Gene 70*, 161−169.
18. Rawlings, M., and Cronan, J. E., Jr. (1992) *J. Biol. Chem. 267*, 5751−5754.
19. Rawlings, M. (1993) Ph.D. Thesis, University of Illinois, Urbana-Champaign, IL.
20. Trent, M. S., Worsham, L., and Ernst-Fonberg, M. L. (1999) *Biochemistry 38*, 3433−3439.
21. Sanger, F., Nicklen, S., and Coulson, A. R. (1977) *Proc. Natl. Acad. Sci. U.S.A. 74*, 5463−5467.
22. Trent, M. S., Worsham, L., Ernst-Fonberg, M. L. (1999) *Biochemistry 38*, 9541−9548.
23. Worsham, L. M. S., Williams, S., and Ernst-Fonberg, M. L. (1993) *Biochim. Biophys. Acta 1170*, 62−71.
24. Alberts, A. W., and Vagelo, P. R. (1961) *Fed. Proc. 20*, 273−284.

25. Worsham, L. M. S., Tucker, M. M., and Ernst-Fonberg, M. L. (1988) *Biochim. Biophys. Acta 963*, 423−428.
26. Bradford, M. M. (1976) *Anal. Biochem. 72*, 748−754.
27. Smith, P. K., Krohn, R. I., Hermanson, G. T., Malliam, A. K. Gartner, F. H., Provenzano, M. D., Fujimato, E. K., Goeke, N. M., Olson, B. J., and Klenk, D. C. (1985) *Anal. Biochem. 150*, 76−85.
28. Laemmli, V. (1970) *Nature 227*, 680−685.
29. Post-Beittenmiller, D., Jaworski, J. G., and Ohlrogge, J. B. (1991) *J. Biol. Chem. 266*, 1858−1865.
30. Young, L., Jernigan, R. L., and Covell, D. G. (1994) *Protein Sci. 3*, 717−729.
31. Lakowicz, J. R. (1999) *Principles of Fluorescence Spectroscopy*, 6th ed., pp 298−310, Kluwer Academic/Plenum Publishers, New York.
32. Haugland, R. P. (1996) *Handbook of Fluorescent Probes and Research Chemical*, 6th ed., p 56, Molecular Probes Inc., Eugene, OR.
33. Eftink, M. R., and Ghiron, C. A. (1976) *Biochemistry 15*, 672−680.
34. Zhang, Y.-M., Rao, M. S., Heath, R. J., Price, A. C., Olson, A. J., Rock, C. O., and Whiate, S. W. (2001) *J. Biol. Chem. 276*, 8231−8238.
35. Jackowski, S., and Rock, C. O. (1987) *J. Bacteriol. 169*, 1469−1473.
36. de la Roche, M. A., Shen, S. S., Zaiwei, K..H., and Byers, D. M. (1997) *Arch. Biochem. Biophys. 344*, 159−164.
37. Hiratsuka, T. (1992) *J. Biol. Chem. 267*, 14941−14948.
38. Parris, K. D., Lin, L., Tam, A, Mathew, R, Hixon, J., Stahl, M., Fritz, C. C., Seehra, J., and Somers, W. S. (2000) *Structure 8*, 883−895.
39. Hill, R. B., and Prestegard, J. H. (1995) *A NMR Approach to the Study of Protein−Protein Interactions: The Interaction of 4-fluorodecanoyl-Acyl-Carrier Protein with Bloch Dehydrase*, Ph.D. Thesis/Dissertation, Yale University, New Haven, CT.
40. Flaman, A. S., Chen, J. M., Van Iderstine, S. C., and Byers, D. M. (2001) *J. Biol. Chem. 276*, 35934−35939.

BI0261950